Frontier orbital interactions in the hetero Diels–Alder cycloaddition of diazadienes

Pratibha Sharma, Ashok Kumar, Vinita Sahu, and Jitendra Singh

Abstract: This work deals with the molecular orbital calculation studies performed on different diazadienes to assess their reactivity pattern. The interaction of these diazadienes with various electron-poor and electron-rich dienophiles leads to the formation of diazines and tetrazines as the cycloadducts. The results from frontier orbital interactions were used to rationalize the reactivity and predictability of NDAC and IEDDAC reaction pathways. Correlation studies were also performed to predict reactivity sequence using a number of electronic descriptors, such as electrophilicity index (ω), chemical potential (μ), electronic charge ΔN_{max}, and chemical hardness η. Moreover, these studies exhibit good compatibility with experimental observations.

Key words: AM1, MNDO, PM3, diazadienes, tetrazines, electrophilicity index, chemical potential.

Résumé : Dans ce travail, on rapporte les résultats obtenus lors de calculs d'orbitales moléculaires effectués sur divers diazadiènes dans le but d'évaluer leur mode de réactivité. L'interaction de ces diazadiènes avec divers diénophiles riches et pauvres en électrons conduit, suivant le cas, à la formation de diazines et de tétrazines comme cycloadduits. On a utilisé les résultats d'interactions d'orbitales frontières pour rationaliser la réactivité et pour vérifier si les voies réactionnelles de cycloaddition de Diels–Alder normale et de cycloaddition de Diels–Alder à demande inversée d'électrons peuvent être utilisées pour les prédire. Utilisant un certain nombre de descripteurs électroniques, tel l'indice du caractère électrophile (ω), le potentiel chimique (μ), la charge électronique (ΔN_{max}) et la dureté chimique (η), on a aussi effectué des études de corrélation pour prédire la séquence de réactivité. De plus, ces études présentent une bonne compatibilité avec les observations expérimentales.

Mots-clés : modèle Austin-1 ("AM1"), négligence modifiée du recouvrement différentiel ("MNDO"), modèle paramétrisé numéro 3 ("PM3"), diazadiènes, tétrazines, indice du caractère électrophile, potentiel chimique.

[Traduit par la Rédaction]

Introduction

The Diels–Alder (1) (DA) reaction is one of the most prominent synthetic strategies in organic chemistry to craft annular compounds from small fragments. The DA reactions of 2-azadienes (2) is a very useful method for providing rapid access to a range of highly substituted biologically active heterocyclic system like pyridines, dihydropyridines, and tetrazine (3). The development of synthetic methodologies based on aza-DA reactions to obtain six-membered tetrazines has attracted much interest because of their utility in the field of medicinal chemistry as antitumor drugs and in energetic chemistry as powerful explosives. Hence, the DA reaction is found to be most a promising method for tetrazine synthesis. With the advancement of computational chemistry to predict the fate of a reaction, herein we have tried to incorporate the quantum mechanical results to interpret DA cycloaddition. In this context, the Fukui's FMO method (4) is found to be the most suitable synthetic tool to predict selectivity and reactivity of compounds. A systematic perusal of the literature (5) reveals that the prediction and reactivity of DA reaction are normally based on the strength of HOMO–LUMO interactions between diene and dienophlie. In view of these precedents and as part of our research program devoted to the study of heterocycles (6), we have made an effort to interpret experimental outcomes through normal Diels–Alder cycloaddition (NDAC) and inverse electron-demand Diels–Alder cycloaddition (IEDDAC) pathways. Moreover, we have also incorporated electronic descriptors, such as the electrophilicity index ω, the chemical potential μ, and ΔN_{max}, to interpret cycloaddition reactivity.

A number of diazadienes bearing one or more electron-withdrawing and electron-donating groups have been chosen to initialize these studies using semi-empirical probes (7). These dienes undergo DA reactions with a variety of dienophiles to achieve tetrazines as the final product in appreciable yield under optimum reaction conditions. A judicious selection of the best method to predict the FMO energies of dienes and various dienophiles has been done. A comparative evaluation of different Hamiltonians for various dienes is shown in Table 1, and the AM1 method was found to show good correlation with Fukui's approximations. Hence, we have chosen the AM1 method for further discussion. Moreover, it is to be emphasized here that the MO semi-empirical method allows the study of more complex diazadienes in a very much more facile manner in compari-

Received 29 November 2007. Accepted 19 February 2008. Published on the NRC Research Press Web site at canjchem.nrc.ca on 27 March 2008.

P. Sharma,[1] A. Kumar, V. Sahu, and J. Singh. School of Chemical Sciences, Devi Ahilya University, Takshashila Campus, Indore, MP 452 001, India.

[1]Corresponding author (e-mail: drpratibhasharma@yahoo.com).

 doi:10.1139/V08-035

Table 1. Frontier orbital energies of diazadiene.

	AM1		MNDO		PM3	
Dienes	HOMO	LUMO	HOMO	LUMO	HOMO	LUMO
1	–9.356	0.465	–9.502	0.282	–9.180	0.388
2	–9.903	0.135	–9.982	–0.011	–9.677	0.106
3	–9.998	0.822	–9.691	0.120	–10.157	0.147
4	–9.314	–0.245	–9.310	–0.231	–9.166	–0.552
5	–8.319	–0.036	–9.358	–0.036	–8.544	–0.041
6	–9.794	–1.353	–9.668	–0.915	–9.800	–1.326
7	–8.407	–0.126	–8.812	–0.123	–8.486	–0.501
8	–8.875	–0.237	–8.899	–0.273	–8.864	–0.529
9	–9.456	–0.856	–9.526	–0.327	–9.397	–0.986
10	–9.352	–0.091	–9.440	–0.091	–9.853	–0.574

Fig. 1. Frontier orbital energies for 1,3-butadiene **1**, 2-aza-diene **2**, and diazadiene **3** and **4** (AM1 calculation).

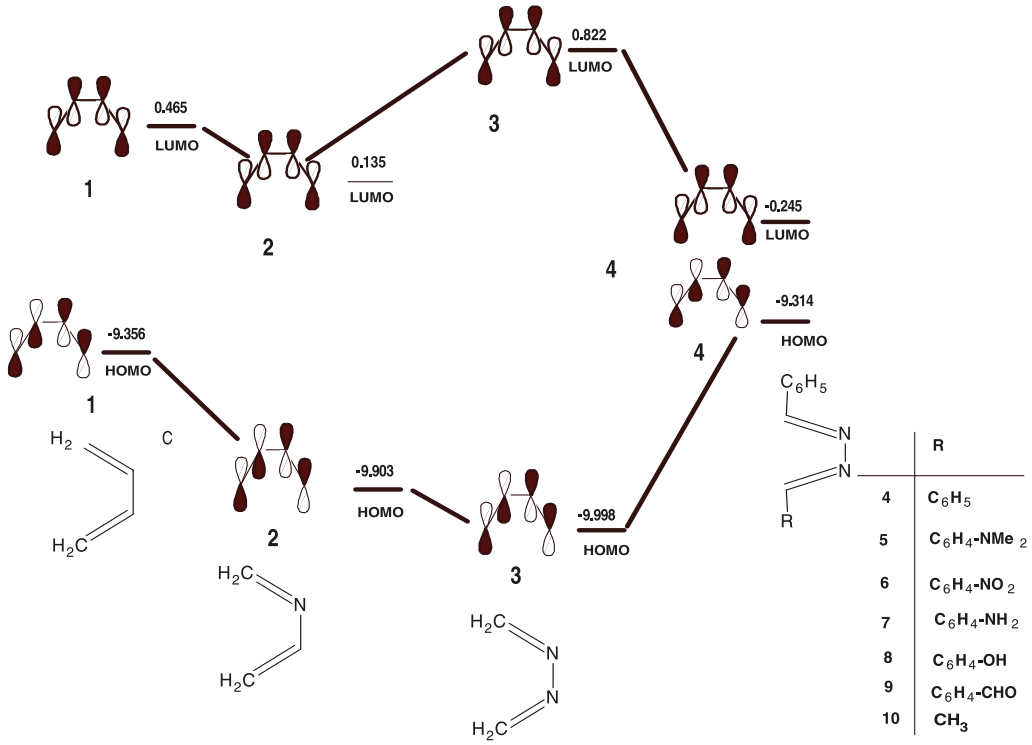

son to ab initio methods. To make a comparative study, we have used some reference dienes and have revealed that 1,3-butadiene (**1**), being an electron-rich diene is prone to undergo NDAC reaction with electron-deficient dienophlie. However, the similar prediction is not easy for heterodienes, because upon substituting one CH moiety of 1,3-butadiene with N, the energy of **2** HOMO–LUMO decreases, while substitution with another N does not show a major decrease in HOMO energy of diene **3** (Figs. 1 and 2).

Furthermore, upon comparing the relative reactivity of diazadienes **4**–**10**, it has been inferred that diazadiene **5**, bearing an electron-donating substituent (i.e., $-NMe_2$) at the phenyl ring, was expected to be more electron-rich compared with **4**, and therefore it is more likely to react with electron-deficient dienophile through the NDAC pathway. On the other hand, **6** takes part in the IEDDAC reaction only with electron-rich dienophile. Similarly, diazadienes **7** and **8**, bearing electron-donating substituents, also show the precedence of the NDAC pathway over IEDDAC with electron-deficient dienophile.

The CH→N substitution in the dienes enhances their reactivity towards electron-rich dienophiles in IEDDAC reactions. However, further decreases in electrophilicity by electron-withdrawing substituent, as in **9** and **6**, makes them more favored species for IEDDAC reactions.

Also, in an attempt to synthesize tetrazines, reference diene **4** was allowed to react with a number of dienophiles **11**–**20** (Figs. 3 and 4) and the experimental results were correlated with theoretical outcomes. The AM1 optimized geometry of cycloadduct **25** is depicted in Fig. 5.

Fig. 2. HOMO and LUMO pictures of dienes **1–3**.

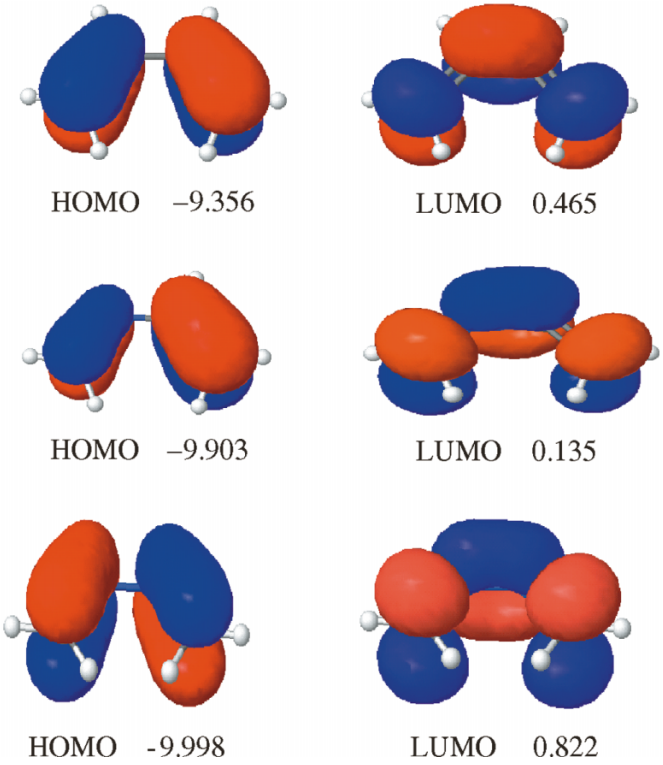

Reactivity of diazadienes 4–10

Table 1 shows the frontier orbital energies of diazadienes **4–10** calculated at the AM1 level. The AM1 calculations described above were performed considering the *S-cis* conformations of dienes.

It is deduced from the aforementioned discussion that HOMO–LUMO energies lowers upon CH→N substitution, making them more reactive species towards electron-rich dienophiles. Substitution of an electron-donating group (–NMe_2) at the phenyl ring raises the HOMO energy by 0.995 eV and lowers the LUMO energy, thereby explaining their preferred participation in NDAC reactions. The calculated HOMO energies of **4**, **6, 9**, and **10** are lower than those of **5**, **7**, and **8**. This explains the lack of reactivity of these diazadienes towards electron-deficient dienophiles (NDAC). On the other hand, the predicted LUMO energies of **4**, **6–10** are lower than that of **5**, pointing to an increased reactivity toward electron-rich dienophiles (IEDDAC). Diazadienes **6**, bearing a nitrophenyl group, has the lowest energy followed by **9**, **10**, and **4**. This indicates that the addition of one nitro group at the 4-position of phenyl ring of diazadienes has a more substantial effect than the introduction of N at the same position.

It can be concluded that on the basis of HOMO energy from AM1 calculations, the reactivity of different diazadienes to participate in inverse electron-demand DA reactions would be in the following order: **6** > **9** > **10** > **4** > **8** > **7** > **5**.

NDAC and IEDDAC

In a view to unravelling the understanding of the mechanistic details of DA cycloaddition, we have taken the Fukui's assumption into consideration and tried to associate the experimental results with computational semi-empirical outcomes. Hence to gain deeper insight into the DA cycloaddition strategy, we proceeded with the treatment of diazadiene **4** with different dienophiles **11–20** and the pertinent results are presented in Tables 2 and 3.

Here we offer an interesting and novel interpretation of eigenfunctions to predict the outcomes of DA reactions. In this context, diazadiene **4**, which is an electron-rich diene, shows similar reactivity with maleic anhydride **16**, bis-4-nitrophenyl diazene **19**, and 4-[4-nitrophenyl]-diazenyl phenol **20**, which are electron-deficient dienophiles. The reaction time required for **4** and dienophiles **16**, **19**, and **20** was found to be approximately similar, favoring NDAC pathway. Moving toward more electron-rich dienophiles, other than **16**, **19**, and **20**, the reaction time increases and sometimes no reaction occurs. 1,2-Ethoxyethene **11** and allyl chloride **18** should take the longest time for reaction with **4**. In actuality, the reactions of **4** with allyl halide **18** requires 13 h, which may be due to the high HOMO–LUMO energy gap for this NDAC reaction, which includes a significant molecular orbital energy gap. A close inspection of eigenfunctions suggests that the dienophile 1,2-ethoxyethene **11**, *N*,*N*-dimethy-4-phenyldiazenyl aniline **12**, and 4-phenyldiazenyl aniline **13**, are likely to undergo IEDDAC reaction, and the experimental results show that dienophiles **11** and **12**, being highly electron-rich dienophiles, remain unreactive with diene **4** after a long time. According to the energy level gap between participating molecular orbitals for dienophiles **12** and 1**3**, both are prone to undergo the IEDDAC pathway, but experimentally no reaction occurs with diazadiene **4** under similar reaction conditions. With dienophile 4-phenyldiazenyl phenol **14**, 1-(dinitrophenyl)-2-phenyldiazene **15**, and diethyl fumarate **17**, reactions proceed according to our expectations, and the experimental results are in agreement with computational outcomes with nearly similar reactivity. It has been experimentally found that the normal DA cycloaddition of diazadiene **4** with allyl chloride **18** provides better yield of the adduct, although the HOMO–LUMO energy gap is larger for these reactions, in contrast with other cycloadditions.

Discussion

A perusal of the calculated energies (Table 2) of the frontier orbitals for the diazadiene **4** and the dienophile points out the significance of the HOMO–LUMO energy gap (Fig. 6). Here Lde-Hdo represents the calculated energy gap (eV) between each dienophile with respect to the LUMO of diene **4**. Ldo-Hde represents the calculated energy gap (eV) between the dienophile's LUMO with respect to the HOMO of diene **4**. The Ldo-Hde energy gap is least (7.695 eV) for diazadiene **4** and maleic anhydride **16**. As **16** is an electron-deficient dienophile, this energy gap favors the NDAC reaction, while the highest energy gap for 1,2-ethoxyethene **11** makes this reaction IEDDAC. Furthermore, it is interesting to note that the energy gap (Lde-Hdo) between diazadiene **4** and *N*,*N*-dimethy-4-phenyldiazenyl aniline **12**, and 4-phenyldiazenyl aniline **13** and 4-phenyldiazenyl phenol **14** dienophiles, are nearly similar, but their reactivities differ markedly, which further emphasizes that the Lde-Hdo en-

Fig. 3. Orbital energies (eV) and geometries of dienophile **11**–**20**.

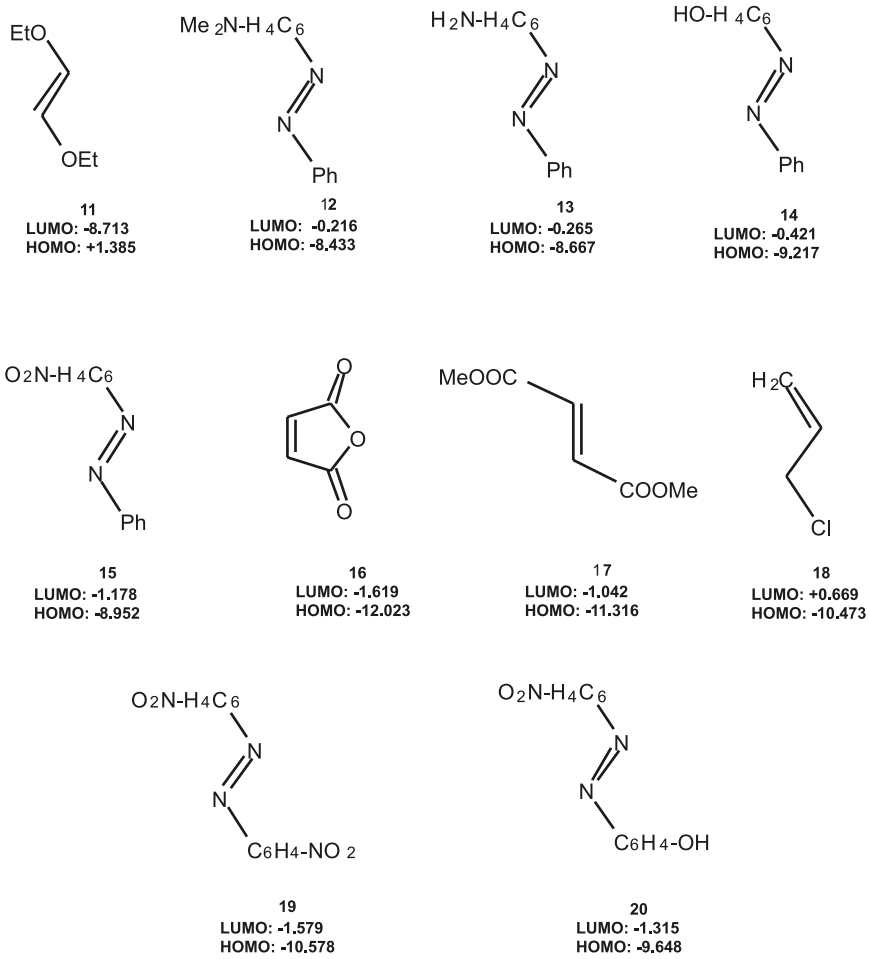

ergy gap is not a reliable tool to predict the reactivity of dienes and dienophiles toward IEDDAC reactions. However, the Ldo-Hde energy gap reasonably predicts the reactivity of dienes and dienophiles. Hence, the NDAC is a more favored pathway for DA reactions than is IEDDAC.

Global electrophilicity index

For a long time Domingo's group has been interested in the study of the molecular mechanism of the polar DA reactions (8–9). Recently, the use of the global electrophilicity index ω proposed by Parr et al. (10), has been reported to classify the global electrophilicity of a series of dienes and dienophiles currently present in DA reactions (11). We found a good correlation between the difference in electrophilicity for the diene and dienophile pair, Δω, and the feasibility of the cycloaddition. Therefore, Δω for a diene–dienophile pair is a valuable tool to predict the polar character of a DA reaction. The global electrophilicity index ω, which measures the stabilization in energy when the system acquires an additional electronic charge N_{max} from the environment, has been given the following simple expression,

$$\omega = \mu^2/2\ \eta$$

where $\mu \approx (I + A)/2$ and $\eta = (A - I)$ are the electronic chemical potential and chemical hardness of the ground state of atoms and molecules, respectively, approximated in terms of the vertical ionization potential (I) and electron affinity (A) using Koopman's theorem. Here, in our calculations $I = E_{HOMO}$ and $A = E_{LUMO}$ were used.

The electrophilicity index encompasses both the propensity of the electrophile to acquire an additional electronic charge driven by μ^2 (the square of the electronegativity) and the resistance of the system to exchange electronic charge with the environment described by η simultaneously. The maximum electronic charge N_{max} is another useful quantity; it is the maximal electronic charge which electron accept from environment, giving a better understanding of Fukui's model.

Table 4 presents an overview of electronic parameters such as electronic chemical potential μ, chemical hardness η, and global electrophilicity index ω. The electronic chemical potential for dienophile **11**–**20** lies in the range –6.821 to –3.664, whereas for diene **4** this value is an intermediate one, –4.779. Dienophiles**11**, **12**, and **13** have higher chemical potentials than **4**, which further suggests that a net charge transfer will take place from electron-rich dienophiles to electron-poor diene **4** in an IEDDAC reaction pathway. In addition, a good correlation can be observed between the substitution pattern on dienophile and the chemical potential μ for the remaining dienophiles **14**–**20**, where charge transfer take place from an electron-rich diene to an electron-deficient dienophile through the NDAC pathway.

Fig. 4. Various cycloadducts **21**–**30**.

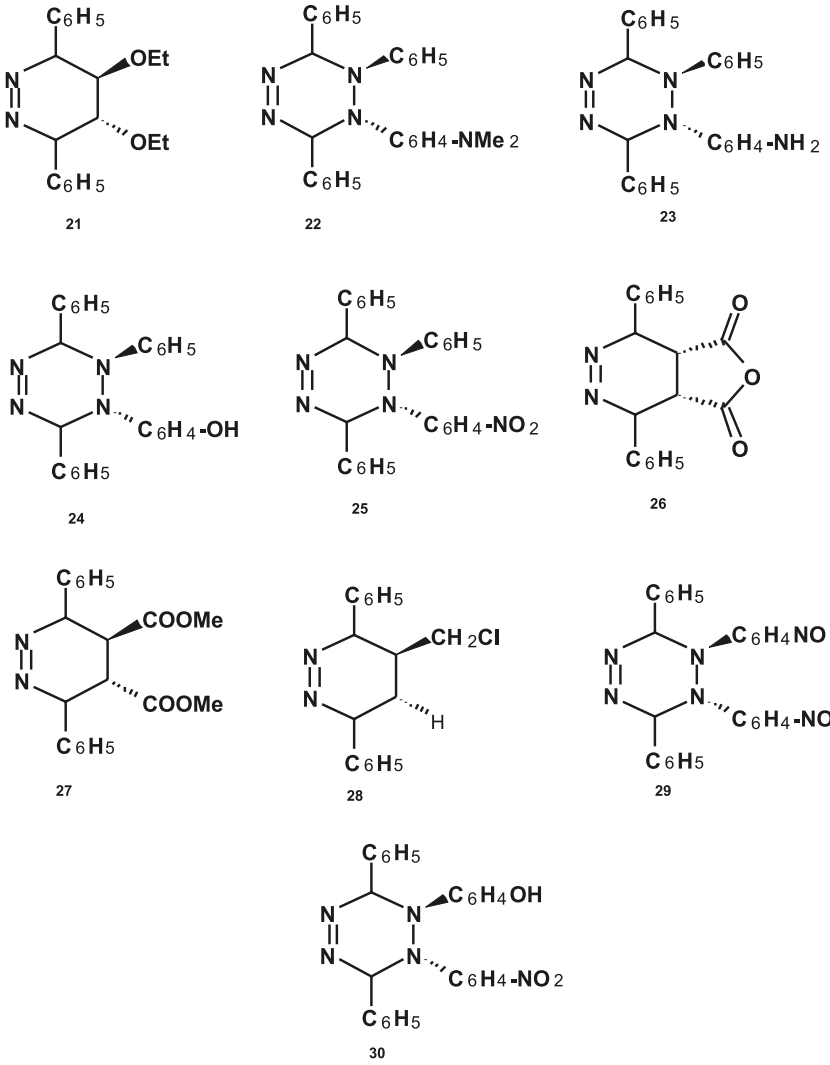

Fig. 5. Optimized geometry of tetrazine cycloadduct **25**.

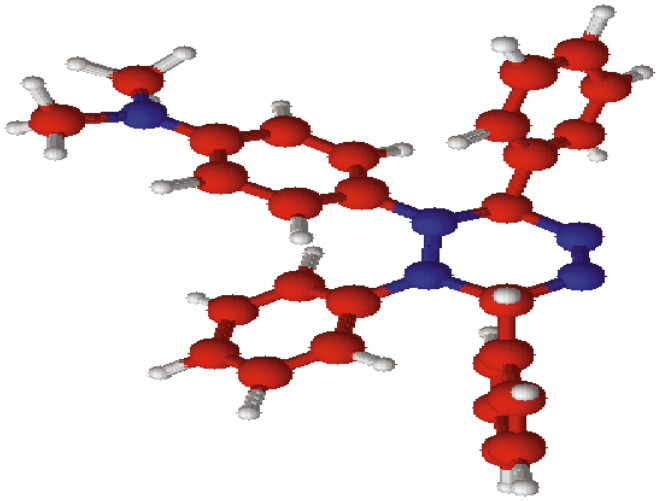

The μ value is found to be lowest for **16** amongst dienohiles **11**–**20**, indicating ease of reaction with the least Ldo-Hde energy gap (7.695) in DA cycloaddition. Experimentally this reaction took the least reaction time to completion (~2 h) in the presence of xylene.

The highest μ value of –3.664 for **11** opens up the possibility of an inverse electron-demand DA reaction in which charge transfer direction is from an electron-rich dienophile to an electron-deficient diene, making this reaction experimentally not feasible under similar reaction conditions. The electrophilicity index ω values for the diene and dienophile falls within the range 18.08–60.84 eV; the highest ω value obtain for **16** illustrates the highly electrophilic nature of this dienophile and is supported by experimental observations. Moreover, the difference in electrophilicity between the diazadiene **4** and dienophiles (Δω) gives a measure of the reactivity of diene and dienophiles in a cycloaddition reaction, where the smallest value of Δω for dienophile **16** suggests the nonpolar synchronous nature of transition states in normal DA cycloaddition.

On the other hand, the highest Δω difference value for the **4a+1** reaction provides an asynchronous polar transition state and IEDDAC pathway, which is experimentally not observable and no reaction occurs at all.

Table 2. Calculated HOMO and LUMO energies of diazadiene **4** and dienophiles **11**–**20**.

S. No.	Diene–dienophile	HOMO	LUMO	Ldo-Hde	Lde-Hdo
1	4	–9.314	–0.245	9.069	9.069
2	11	–8.713	1.385	10.699	8.468
3	12	–8.433	–0.216	9.098	8.188
4	13	–8.667	–0.265	9.049	8.422
5	14	–9.215	–0.421	8.893	8.970
6	15	–8.952	–1.178	8.136	8.707
7	16	–12.023	–1.619	7.695	11.778
8	17	–11.316	–1.042	8.272	11.071
9	18	–10.473	0.669	9.983	10.228
10	19	–10.578	–1.579	7.735	10.333
11	20	–9.648	–1.315	7.999	9.403

Table 3. Experimental results of the **[4+2]** cycloaddition of diene **4** with dienophiles **11**–**20**.

Entry	Dienophile	Adduct	Time to completion (h)	Yield (%)
1	11	21	—	—
2	12	22	—	—
3	13	23	—	—
4	14	24	20	65
5	15	25	8	70
6	16	26	2	85
7	17	27	6.5	75
8	18	28	13	70
9	19	29	4	79
10	20	30	6	78

Fig. 6. Molecular orbital energy gap between diene **4** and dienophile **11** and **16**.

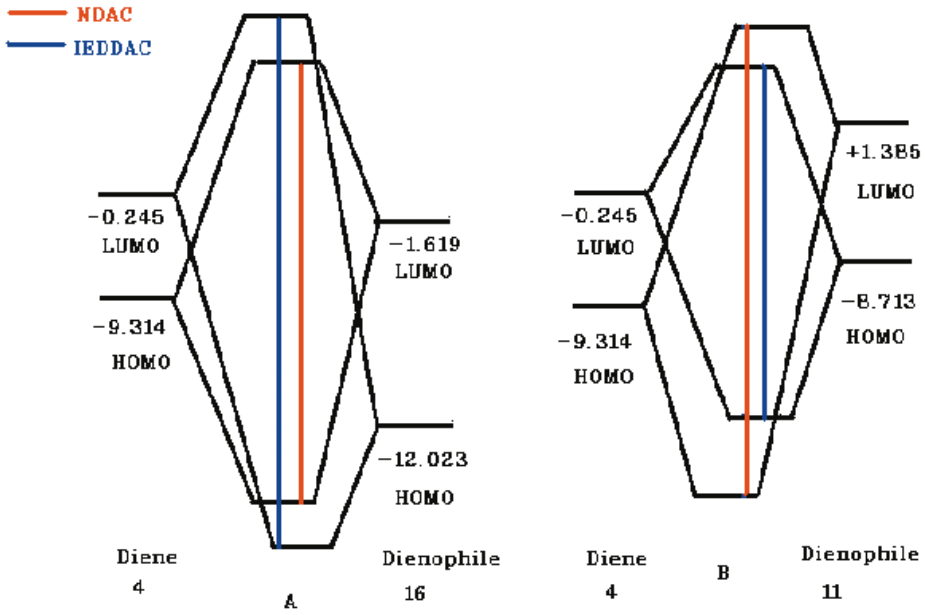

Multiple analysis regression (MAR) data between the electrophilicity index ω and electron affinity EA for 11 compounds (Table 4) shows that the statistical parameters (standard deviation) SD ≈ 0.31 and (correlation co-efficient) $R \approx 0.95$ significantly support excellent correlation (Fig. 7) between the electrophilicity index ω and electron affinity EA.

The stereo- and regio-selectivity of DA cycloadditions are easily rationalized by examining the orbital coefficient values on the molecular orbitals. The preferred regioisomeric transition states in DA cycloadditions depends upon the terminal coefficient of the interacting orbitals. Table 5 shows the orbital coefficient at different carbon atoms of dienes **1**–

Table 4. Global electronic descriptors values of diene and dienophiles.

Entry	Diene/dienophile	HOMO	LUMO	μ (a.u.)	η (a.u.)	ω (eV)	N_{max}	ω (eV)
1	4	–9.314	–0.245	–4.779	9.069	34.26	0.527	0.00
2	11	–8.713	+1.385	–3.664	10.098	18.08	0.363	+16.180
3	12	–8.433	–0.216	–4.324	8.217	30.95	0.526	+3.310
4	13	–8.667	–0.265	–4.466	8.402	32.30	0.532	+1.960
5	14	–9.215	–0.421	–4.818	8.794	35.91	0.548	–1.650
6	15	–8.952	–1.178	–5.065	7.774	44.90	0.652	–10.640
7	16	–12.023	–1.619	–6.821	10.404	60.84	0.656	–26.580
8	17	–11.316	–1.042	–6.179	10.274	50.56	0.601	–16.300
9	18	–10.473	+0.669	–4.902	11.142	29.34	0.440	+4.920
10	19	–10.578	–1.579	–6.078	8.999	55.86	0.675	–21.600
11	20	–9.648	–1.315	–5.482	8.333	49.05	0.660	–14.790

Fig. 7. Correlation graph vs. electrophilicity index ω and electron affinity EA.

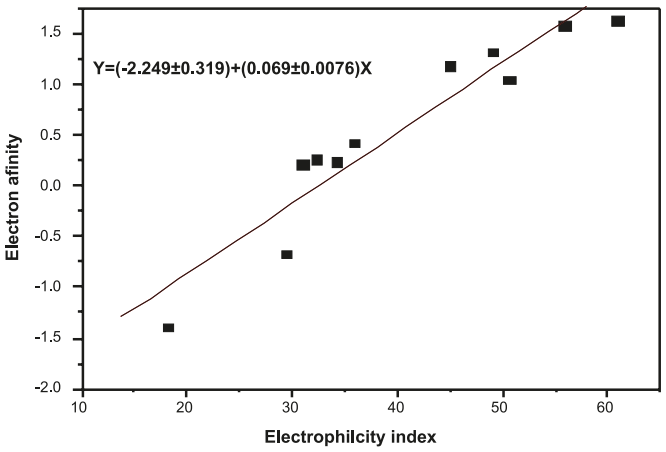

4 and **10**. The results demonstrate that in 1,3-butadiene **1**, the terminal coefficient at C-1 and C-4 of HOMO wave functions are of equal magnitude, but upon CH→N substitution the coefficient magnitude suddenly decreases and so 1-azadienes becomes regiospecific for the unsymmetrical substituted dienophile. Introduction of N in 1,3-butadiene enhances the electrophilicity of the diene, making it a preferred species for IEDDAC reaction. In azadienes, the C-1 position is more polarized than the C-4 position. A similar decrease in orbital coefficient is found upon introducing another N in the diene moiety. A close examination of the orbital coefficients on azadienes **2** and **3** reveals that the magnitude of the orbital coefficients is larger on the C-3/N-3 position than on the C-2/N-2 position, which could play an immense role in the preferred formation of regioisomers through secondary orbital interactions.

An exhaustive exploration of orbital coefficients on different dienophiles (Table 6) provides regioselective understanding toward the DA cycloadduct. The orbital coefficients of the symmetrical molecule (dienophile) are identical in magnitude at terminal atomic centers. These studies show that **D-1** (here **D-1** is taken as reference dienophile to interpret the comparative results of dienophiles **11**–**20** in terms of orbital coefficients, C_6H_5-N=N-C_6H_5) has a similar orbital coefficient at N-1 and N-2 in LUMO, while these values are considerably lower due to the electron-withdrawing phenyl substituent, which makes this species more electron-withdrawing and favorable for NDAC reactions. 1-(Dinitrophenyl)-2-phenyldiazene **15** and 4-[4-nitrophenyl]-diazenyl phenol **20**, having at least one electron-withdrawing moiety attached to the phenyl ring, show the low orbital coefficient at N-2, which is in accordance with literature data. Similarly, 4-phenyldiazenyl aniline **13** and 4-phenyldiazenyl phenol **14**, having electron-releasing substiutents at the phenyl ring, possess larger orbital coefficients at N-1 than at N-2, making these species regiospecific towards unsymmetrical dienes. However, similar predictions cannot be made for *N*,*N*-dimethy-4-phenyldiazenyl aniline **12**, which remains unreactive in DA cycloaddition with diazadiene **4**.

Regioselective studies

When an unsymmetrical diene **10** is allowed to react with a certain range of the aforementioned unsymmetrical dienophiles, the regioselectivity of the cycloadduct was also taken into consideration. We have calculated atomic orbital coefficients at interacting orbitals to check their participation in DA cycloaddition. The orbital coefficient values on diazadienes are very much lower than for their carbon congeners. A close inspection of the coefficients of diene **10** and dienophlie **15** suggest the preferred formation of regioselective **R-31b** over **R-31a**. The experimental results were in accordance with these findings. For a better understanding of regioselectivty in hetero DA reactionsm, diene **10** was also treated with dienophile **20** and preferred formation of **R-32a** rather than **R-32b** was in support of Houk's assumption. Both of these reactions follow the NDAC pathway under similar reaction conditions (Fig. 8).

Furthermore, the role of secondary orbital interactions in deciding the regioselectivity of the product was also envisaged in the case of unsymmetrical diene **10**. It has been revealed that when diazadiene **10** was allowed to react with dienophile **15**, **R-31b** was solely obtained as the regioselective cycloadduct because of primary orbital interactions between terminal orbital coefficients of the HOMO diene and the LUMO dienophile. It has been noticed that preferred regioisomers can still be predicted by considering secondary orbital interactions between the N-2 and N-3 positions of diene **10** and the C_6H_4-NO_2 moiety of dienophlie **15**. A close inspection of the orbital coefficients at N-2 and N-3 in diene **10** show that N-2 has higher orbital coefficient than N-3. Thus, the stabilization of an endo transition state is greater when the C_6H_4-NO_2 group of dienophile **15** is near

Table 5. Orbital coefficient values at different diazadienes.

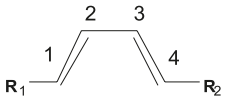

	R_1	R_2
1	H	H
2	H	H
3	H	H
4	Ph	Ph
10	Ph	CH_3

	Orbital coefficient (HOMO)				Orbital coefficient (LUMO)			
Diene	C-1	C-2/N-2	C-3/N-3	C-4	C-1	C-2/N-2	C-3/N-3	C-4
1	0.563	0.427	0.427	0.563	0.566	0.423	0.423	0.566
2	0.328	0.219	0.406	0.550	0.579	0.439	0.368	0.579
3	0.306	0.118	0.391	0.199	0.511	0.4354	0.012	0.021
4	0.230	0.243	0.241	0.044	0.333	0.395	0.030	0.056
10	0.028	0.065	0.038	0.069	0.030	0.081	0.041	0.071

Table 6. Orbital coefficient values at different dienophiles.

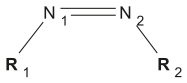

	R_1	R_2
D-1	Ph	Ph
12	Ph	Ph-NMe_2
13	Ph	Ph-NH_2
14	Ph	Ph-OH
15	Ph	Ph-NO_2
20	Ph-OH	Ph-NO_2

	Orbital coefficient (HOMO)		Orbital coefficient (LUMO)	
Dienophile	N-1	N-2	N-1	N-2
D-1	0.119	0.102	0.388	0.370
12	0.164	0.056	0.372	0.293
13	0.189	0.068	0.403	0.332
14	0.146	0.115	0.403	0.327
15	0.125	0.114	0.071	0.024
20	0.059	0.317	0.366	0.278

the secondary position of the diene, yielding the **R-31b** isomer as the favourable product.

Upon similar analysis, the regioselective formation of **R-32a** can be explained by considering the secondary orbital interactions between orbital coefficients at N-2 of diene **10** and the C_6H_4-NO_2 moiety of dienophile **20**. Thus, secondary orbital interactions exerted a significant effect on the regioselectivity of the Diels Alder reaction between unsymmetrically substituted diene and dienophile.

Conclusion

Concluding, we have performed and interpreted FMO interactions with a critical evaluation of the reaction pathways. Highlights of all the studies can be summarized as follows. (*i*) The relative reactivity of different diazadienes in DA reactions was studied in a selective and predictive way. (*ii*) The Ldo-Hde energy gap was found to a be a favored tool to predict DA cycloaddition. These predictions are in good agreement with experimental findings where diene **4** exhibited high reactivity towards **15**, which is a electron-deficient species in NDAC pathway. (*iii*) Synthesis of different substituted tetrazines were achieved via NDAC and IEDDAC DA pathways. (*iv*) All the results were interpreted in terms of electrophilicity index ω and a good correlation was observed between global electronic parameters and experimental findings. Hence, the FMO interactions are the key players to decide the fate of DA reactions. Similar studies on hetero DA reactions are in progress.

Acknowledgements

We are grateful to the Central Drug Research Institute, Lucknow, India for providing spectroanalytical facilities. One of the authors (VS) is also thankful to the Council of Scientific and Industrial Research (CSIR), India, for providing a junior research fellowship.

Experimental

Computational method

The AMl, MNDO, and PM3 approximations to molecular orbital theory have been employed using the MOPAC 2007 computer program (12). The geometries were fully optimized at minimum gradient level (0.01). The minimum energy conformations were used to compute molecular orbital and charge distributions. To explain the results in terms of global electronic parameters viz., electrophlicity index ω, chemical potential μ, etc., the calculations were done at MOPAC 2007 program.

General

All the chemicals used were of AR grade purity. IR spectra were recorded on PerkinElmer model 377 spectrophotometer in KBr pellets. ^{1}H NMR spectra were recorded on a Bruker DRX300 instrument. The FAB mass spectra were recorded on a JEOLSX102/DA–6000 Mass Spectrometer using argon–xenon (6 kv, 10 mA) as the FAB gas. Analytical thin layer chromatography was performed using E. Merck silica gel G (0.50 mm plates, Merck No. 5700). The melting points were determined on an electric melting point apparatus in open capillaries and are uncorrected.

Fig. 8. Predictions of regioselectivity for diazadiene **10** and dienophiles **15** and **20**.

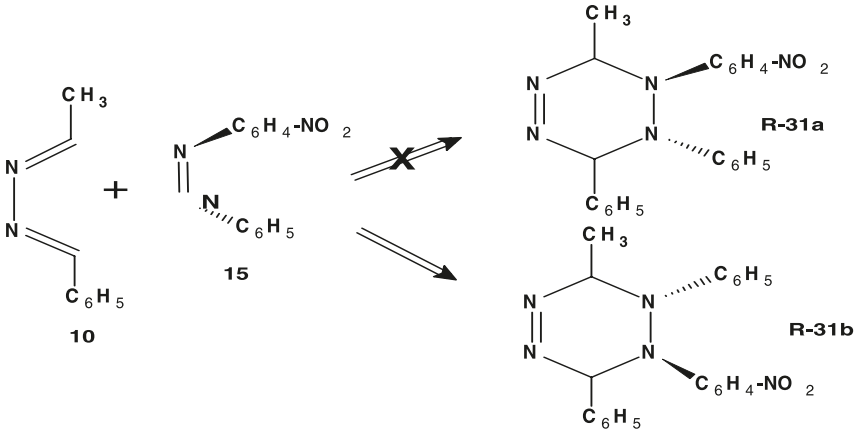

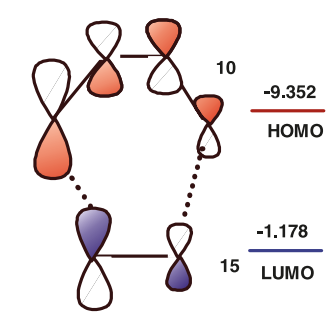

Orbital interactions in diene 10 and dienophile 15 to form R 31b

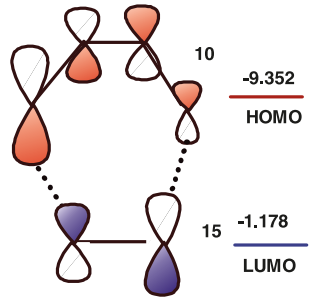

Orbital interactions in diene 10 and dienophile 15 to form R 31a

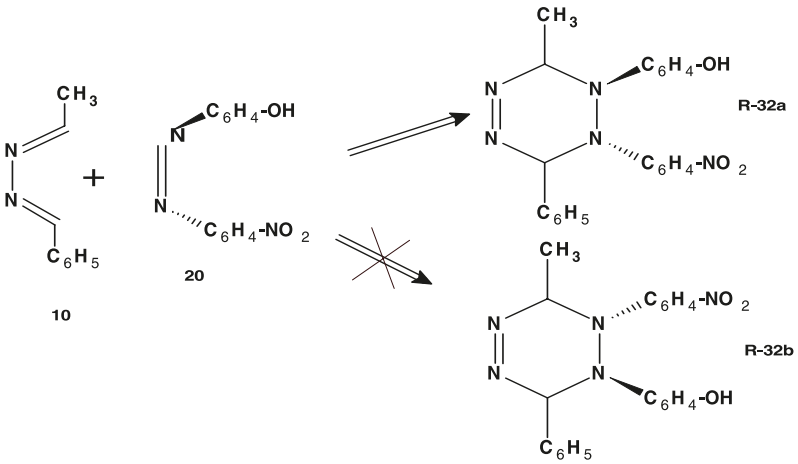

Synthesis of diazadiene 4

The diazadiene **4** was prepared by condensing together dissolving hydrazine hydrate (0.05 mol) into 50% glacial acetic acid (10 mL), and to this solution bezaldehyde (0.10 mol) was added to obtained diazadiene **4** in good yield (80%) as a yellow-green crystalline product. It was washed with cold water and recrystallized from ethanol.

Typical procedure for Diels–Alder reactions

To a solution of diazadiene **4** (0.01 mol) in dry xylene was added dienophile **11**–**20** (0.01 mol) in equimolar quantity. The solution was then refluxed for the required time (Table 3) with constant stirring. At the end of the reaction, solvent were distilled off at reduced pressure from the reaction mixture and the crude cycloadduct was recrystallised and purified by TLC resolution studies on silica gel (E Merck) using ethyl acetate–xylene (4:6, *v*/*v*).

Adduct 24

The reaction was performed according to the general procedure starting with 1.98 gm of **14**. The cycloadduct was isolated in 65% yield, mp 112 °C, decomposed. IR (KBr, cm^{-1}) 3570 (–OH str.), 3033 (=C-H, sp^2), 2986 (C-H, sp^3), 1621 (C=C), 1541 (N=N), 1458, 1371 (C-H, bending, sp^3), 1071 (C-O), 1046 (C-N), 886, 763, 676 (sub. phenyl). ^{1}H NMR (ppm) δ: 3.15 (s, 1H, -CH-Ph), 3.37 (s, 1H, -CH-

Ph), 6.85 (dd, 2H, -C_6H_4-OH, J = 8.5 Hz, J = 2.7 Hz), 7.17 (dd, 2H, –C_6H_4-OH, J = 8.1 Hz, J = 2.8 Hz), 7.21–7.67 (m, 15H, -phenyl), 11.75 (s, 1H, -OH). FAB-MS *m/z*: 407. Anal. calcd. for $C_{26}H_{22}N_4O$: C 76.83, H 5.46, N 13.78; found: C 76.78, H 5.41, N 13.72.

Adduct 25

The reaction was performed according to the general procedure starting with 2.27 gm of **15**. The cycloadduct was isolated in 70% yield, mp 121–122 °C. IR (KBr, cm^{-1}): 3034 (=C-H, sp^2), 2974 (C-H, sp^3), 1623 (C=C), 1544 (N=N), 1535 (–NO_2), 1451, 1361 (C-H, bending, sp^3), 1064 (C-O), 1041 (C-N), 881, 751, 672 (sub. phenyl). ^{1}H NMR (ppm) δ: 3.11 (s, 1H, –CH-Ph), 3.22 (s, 1H, –CH-Ph), 7.45–7.64 (m, 15H, -phenyl), 7.74 (dd, 2H, –C_6H_4-NO_2, J = 8.6 Hz, J = 3.0 Hz), 8.11 (dd, 2H, –C_6H_4-NO_2, J = 9.1 Hz, J = 2.2 Hz). FAB-MS *m/z*: 436. Anal. calcd. for $C_{26}H_{21}N_5O_2$: C 71.71, H 4.86, N 16.08; found: C 71.67, H 4.79, N 16.01.

Adduct 26

The reaction was performed according to the general procedure starting with 0.98 gm of **16**. The cycloadduct was isolated in 85% yield, mp 124–125 °C. IR (KBr, cm^{-1}): 3028 (=C-H, sp^2), 2884 (C-H, sp^3), 1778 (–C=O, anhydride), 1612 (C=C), 1544 (N=N), 1444, 1348 (C-H, bending, sp^3), 1071 (C-O), 1049 (C-N), 761, 688 (sub. phenyl). ^{1}H NMR (ppm) δ: 2.55 (d, 2H, –CH × 2, J = 5.8 Hz), 3.21 (d, 2H, –CH-Ph × 2, J = 6.1 Hz), 6.83–7.81 (m, 10H, –phenyl). FAB-MS *m/z*: 307. Anal. calcd. for $C_{18}H_{14}N_2O_3$: C 70.58, H 4.61, N 9.51; found: C 70.51, H 4.59, N 9.48.

Adduct 27

The reaction was performed according to the general procedure starting with 1.44 gm of **17**. The cycloadduct was isolated in 75% yield, mp 130–132 °C. IR (KBr, cm^{-1}): 3034 (=C-H, sp^2), 2889 (C-H, sp^3), 1771 (–C=O, ester), 1621 (C=C), 1551 (N=N), 1434, 1371 (C-H, bending, sp^3), 1061 (C-O), 1053 (C-N), 775, 669 (sub. phenyl). ^{1}H NMR (ppm) δ: 2.38 (d, 2H, –CH × 2, J = 5.5 Hz), 3.33 (d, 2H, –CH-Ph × 2), 3.80 (s, 6H, –$COOCH_3$), 6.81–7.66 (m, 10H, –phenyl). FAB-MS *m/z*: 353. Anal. calcd. for $C_{20}H_{20}N_2O_4$: C 68.17, H 5.72, N 7.95; found: C 68.14, H 5.67, N 7.89.

Adduct 28

The reaction was performed according to the general procedure starting with 0.76 gm of **18**. The cycloadduct was isolated in 70% yield, mp 78–80 °C. IR (KBr, cm^{-1}): 3032 (=C-H, sp^2), 2891(C-H, sp^3), 1615 (C=C), 1557 (N=N), 1450, 1368 (C-H, bending, sp^3), 550 (C-Cl), 1050 (C-N), 765, 661 (sub. phenyl). ^{1}H NMR (ppm) δ: 2.48 (d, 2H, –CH_2–), 2.61 (d, 1H, –CH-C_6H_5, J = 5.9 Hz), 2.71 (m, 1H, –CH-), 2.78 (d, 1H, –CH-C_6H_5, J = 5.7 Hz), 2.98 (d, 2H, –CH_2-Cl, J = 6.5 Hz), 7.22–7.58 (m, 10H, –phenyl). FAB-MS *m/z*: 285. Anal. calcd for $C_{17}H_{17}ClN_2$: C 71.70, H 6.02, N 9.84; found: C 71.67, H 5.92, N 9.78.

Adduct 29

The reaction was performed according to the general procedure starting with 2.72 gm of **19**. The cycloadduct was isolated in 79% yield, mp 79–80 °C. IR (KBr, cm^{-1}): 3034 (=C-H, sp^2), 2974 (C-H, sp^3), 1623 (C=C), 1544 (N=N), 1535 (–NO_2), 1451, 1361 (C-H, bending, sp^3), 1041 (C-N), 881, 751, 672 (sub. phenyl). ^{1}H NMR (ppm) δ: 3.16 (s, 2H, –CH-Ph × 2), 7.44–7.66 (m, 10H, –phenyl), 7.70 (dd, 4H, –C_6H_4-NO_2, J = 8.5 Hz, J = 2.3 Hz), 8.14 (dd, 4H, –C_6H_4-NO_2, J = 8.8 Hz, J = 2.5 Hz). FAB-MS *m/z*: 481. Anal. calcd. for $C_{26}H_{20}N_6O_4$: C 64.99, H 4.20, N 17.49; found: C 64.91, H 4.18, N 17.45.

Adduct 30

The reaction was performed according to the general procedure starting with 2.43 gm of **20**. The cycloadduct was isolated in 78% yield, mp 128–130 °C. IR (KBr, cm^{-1}): 3556 (–OH str.), 3028 (=C-H, sp^2), 2987 (C-H, sp^3), 1615 (C=C), 1548 (N=N), 1548 (–NO_2), 1467, 1372 (C-H, bending, sp^3), 1061 (C-O), 1044(C-N), 884, 761, 669 (sub. phenyl). ^{1}H NMR (ppm) δ: 3.19 (s, 1H, –CH-Ph), 3.32 (s, 1H, –CH-Ph), 6.78 (dd, 2H, –C_6H_4-OH, J = 7.9 Hz, J = 2.9 Hz), 7.31 (dd, 2H, –C_6H_4-OH, J = 8.1 Hz, J = 3.0 Hz), 7.40–7.63 (m, 10H, –phenyl), 7.75 (dd, 2H, –C_6H_4-NO_2, J = 8.5 Hz, J = 2.8 Hz), 7.91 (dd, 2H, –C_6H_4-NO_2, J = 8.7 Hz, J = 2.9 Hz). FAB-MS *m/z*: 452. Anal. calcd. for $C_{26}H_{21}N_5O_3$: C 69.17, H 4.69, N 15.51; found: C 69.11, H 4.65, N 15.49.

Adduct R-31b

The reaction was performed according to the general procedure starting with 2.27 gm of **15**. The cycloadduct was isolated in 71% yield, mp 110–112 °C. IR (KBr, cm^{-1}): 3033 (=C-H, sp^2), 2981 (C-H, sp^3), 1618 (C=C), 1542 (N=N), 1539 (–NO_2), 1441, 1371 (C-H, bending, sp^3), 1061 (C-O), 1044 (C-N), 880, 749, 671 (sub. phenyl). ^{1}H NMR (ppm) δ: 2.62 (d, 3H, –CH_3), 2.68 (q, 1H, –CH-CH_3), 3.23 (s, 1H, –CH-C_6H_5), 6.91–7.43 (m, 10H, –phenyl), 7.51 (dd, 2H, –C_6H_4-NO_2, J = 8.8 Hz, J = 2.4 Hz), 7.84 (dd, 2H, –C_6H_4-NO_2, J = 8.9 Hz, J = 2.9 Hz). FAB-MS *m/z*: 375. Anal. calcd. for $C_{21}H_{19}N_5O_2$: C 67.55, H 5.13, N 18.76; found: C 67.14, H 5.08, N 18.61.

Adduct R-32a

The reaction was performed according to the general procedure starting with 2.43 gm of **20**. The cycloadduct was isolated as reddish brown solid in 75% yield, mp 135–136 °C. IR (KBr, cm^{-1}): 3549 (–OH str.), 3014 (=C-H, sp^2), 2981 (C-H, sp^3), 1614 (C=C), 1543 (N=N), 1551 (–NO_2), 1457, 1371 (C-H, bending, sp^3), 1059 (C-O), 1041 (C-N), 881, 758, 662 (sub. phenyl). ^{1}H NMR (ppm) δ: 2.30 (d, 3H, –CH_3), 2.53 (s, 1H, –CH-CH_3), 3.32 (q, 1H, –CH-C_6H_5), 6.54 (dd, 2H, –C_6H_4-OH, J = 7.9 Hz, J = 2.9 Hz), 6.79 (dd, 2H, –C_6H_4-OH, J = 8.1 Hz, J = 2.3 Hz), 6.99 (s, 5H, –C_6H_5), 7.75 (dd, 2H, –C_6H_4-NO_2, J = 8.5 Hz, J = 2.8 Hz), 7.92 (dd, 2H, –C_6H_4-NO_2, J = 8.8 Hz, J = 2.7 Hz), 11.16 (s, 1H, –OH) ; FAB-MS *m/z*: 390. Anal. calcd. for $C_{21}H_{19}N_5O_3$: C 64.77, H 4.92, N 17.98; found: C 64.61, H 4.85, N 17.89.

References

1. (*a*) J. Sauer and R. Sustmann. Angew. Chem. Int. Ed. Engl. **19**, 779 (1980); (*b*) K.N. Houk, Y.T. Lin, and F.K. Brown. J. Am. Chem. Soc. **108**, 554 (1986); (*c*) W.T. Borden, R.J. Loncharich, and K.N. Houk. Annu. Rev. Phys. Chem. **39**, 213 (1988).

2. (*a*) D.L. Boger, S.R. Duff, J.S. Panek, and M. Yasuda. J. Org. Chem. **50**, 5790 (1985); (*b*) D.L. Boger, J. Schumacher, M.D. Mullican, M. Patel, and S.Panek, J. Org. Chem. **47**, 2673 (1982); (*c*) H. Neunhoeffer and M. Bachmann. Chem. Ber. **108**, 3877 (1975); (*d*) D.L. Boger, R.S. Coleman, J.S. Panek, and D. Yohannes. J. Org. Chem. **49**, 4405 (1984); (*e*) D.L. Boger, R.S. Coleman, J.S. Panek, F.X. Huber, and J. Sauer. J. Org. Chem. **50**, 5377 (1985); (*f*) D.L. Boger and J.S. Panek. Tetrahedron Lett. **24**, 4511 (1983).
3. (*a*) D.L. Boger, D.R. Soenen, C.W. Boyce, M.P. Hedrick and Q. Jin. J. Org. Chem. **65**, 2479 (2000); (*b*) D.L. Boger and S.E. Wolkenberg. J. Org. Chem. **65**, 9120 (2000); (*c*) D.L. Boger and J. Hong. J. Am. Chem. Soc. **123**, 8515 (2001); (*d*) A. Hamasaki, J.M. Zimpleman, I. Hwang, and D.L. Boger. J. Am. Chem. Soc. **127**, 10767 (2005).
4. (*a*) K. Fukui. Acc. Chem. Res. **4**, 57 (1971); (*b*) R.B. Woodward and R. Hoffmann. J. Am. Chem. Soc. **87**, 4388 (1965); see also the review: R.B. Woodward and R. Hoffmann. The conservation of orbital symmetry. Verlag Chemie, Weinheim, Germany. (1970); (*c*) G. Klopmann. J. Am. Chem. Soc. **90**, 223 (1968); (d) L. Salem, J. Am. Chem. Soc. **90**, 543, 553 (1968).
5. (*a*) G. Ujaque, J.E. Norton, and K.N. Houk. J. Org. Chem. **67**, 7179 (2002); (*b*) L.R. Domingo, M.J. Aurell, M. Arno, and J.A. Saez, J. Org. Chem. **72**, 4220 (2007); (*c*) A. Zhong, C. Rong, and S. Liu. J. Phys. Chem. A, **111**, 3132 (2007); (*d*) D.H. Ess and K.N. Houk. J. Am. Chem. Soc. **129**, 10646 (2007); (*d*) P.R.Campodonico, P. Fuentealba, E.A.Castro, J.G. Santos, and R. Contreras. J. Org. Chem. **70**, 1754 (2005).
6. (*a*) P. Sharma, A. Kumar, and P. Pandey. Phosphorous Sulfur Silicon Relat. Elem. **178**, 583 (2003); (*b*) P. Sharma, A. Kumar, and A. Mandloi. Synth. Commun. **33**, 3 (2003); (*c*) P. Sharma, S. Sharma, and N. Rane. Biorg. Med. Chem. **12**, 3135 (2004); (*d*) P. Sharma, A. Kumar, and M. Sharma. Eur. J. Med. Chem. **41**, 883 (2006); (*e*) P. Sharma, N. Rane, and P. Pandey. Archiv. Pharm. **339**, 572 (2006); (*f*) P. Sharma, A. Kumar, N. Rane, and V. Guarram. Tetrahedron, **61**, 4237 (2005).
7. (*a*) M.J.S. Dewar, S. Olivella, and H.S. Rzepa. J. Am. Chem. Soc. **100**, 56 (1978); (*b*) M. Ortega, A. Oliva, J.M. Lluch, and J.Bertran. Chem. Phys. Lett. **102**, 317 (1983); (*c*) F.K. Brown and K.N. Houk. Tetrahedron Lett. **25**, 4609 (1985).
8. (*a*) L.R. Domingo, R.A. Jones, M.T. Picher, and J. Sepulveda Arques. Tetrahedron, **51**, 8739 (1995); (*b*) L.R. Domingo, M.T. Picher, J. Andres, and V.S. Safont. J. Org. Chem. **62**, 1775 (1997); (*c*) L.R. Domingo, M. Arno, and J. Andres. J. Org. Chem. **64**, 5867 (1999); (*d*) L.R. Domingo. Theor. Chem. Acc. **104**, 240 (2000); (*e*) L.R. Domingo. J. Org. Chem. **66**, 3211 (2001).
9. (*a*) L.R. Domingo, M.T. Picher, J. Andres, V. Moliner, and V.S. Safont. Tetrahedron, **52**, 10693 (1996); (*b*) L.R. Domingo, M.T. Picher, and R.J. Zaragoza. J. Org. Chem. **63**, 9183 (1998); (*c*) L.R. Domingo, M.T. Picher, and M.J. Aurell. J. Phys. Chem. A, **103**, 11425 (1999); (*d*) L.R. Domingo, M. Oliva, and J. Andres. J. Org. Chem.**66**, 6151 (2001); (*e*) L.R. Domingo, J. Andres, and C.N. Alves. Eur. J. Org. Chem. 2557 (2002).
10. R.G. Parr, L. Von Szentpaly, and S. Liu. J. Am. Chem. Soc. **121**, 1922 (1999).
11. L.R. Domingo, M.J. Aurell, P. Perez, and R. Contreras. Tetrahedron, **58**, 4417 (2002).
12. MOPAC2007-DS-DG1, ©2007, Stewart Computational Chemistry.